View Journal

JAAS

Journal of Analytical Atomic Spectrometry

Accepted Manuscript

This article can be cited before page numbers have been issued, to do this please use: L. Ripoll and M. Hidalgo Núñez, *J. Anal. At. Spectrom.*, 2019, DOI: 10.1039/C9JA00145J.

Electrospray deposition followed by laser-induced breakdown spectroscopy (ESD-LIBS): a new method for trace elemental analysis in aqueous samples

L. Ripoll* and M. Hidalgo*

Department of Analytical Chemistry and Food Science and University Materials Institute, University of Alicante, Apdo. 99, Alicante E-03080, Spain

Abstract

The combination of electrospray deposition with laser-induced breakdown spectroscopy (ESD-LIBS) was investigated as a potential approach to the detection and quantification of Zn, Cd, Cr and Ni, at trace levels, in aqueous samples. In this analytical procedure, the aqueous samples were first converted into solid in an electrospray system. To this end, micro-volumes of liquid were electro-sprayed onto a heated substrate, leading to the generation of solid residues. Afterwards, the so obtained residues were analysed by LIBS. Three calibration methodologies were tested with the proposed ESD-LIBS methodology, namely external calibration, conventional standard addition calibration and on-line standard addition calibration. In all cases, the analytical features of the ESD-LIBS method were assessed. The obtained limits of detection ranged from 9 μg kg^{-1} to 57 μg kg^{-1}, depending on the element and on the calibration modality used. Method trueness, evaluated from the analysis of a real sample of tap water, was highly dependent on the calibration method. The use of external calibration led to recovery values in the range 15%-123%, indicating the existence of strong matrix effects. This drawback was solved with the application of conventional standard addition and on-line standard addition calibration modalities, for with recovery values were improved to the ranges 91%-110% and 90%-105%, respectively. Among them, the use of on-line standard addition provides a sensitive and accurate methodology with possibilities of automation.

Keywords: LIBS; electrospray deposition; liquid samples, trace analysis.

* Corresponding authors. Tel.: +34 965903400 (Ext. 2421)
E-mail addresses: montserrat.hidalgo@ua.es (M. Hidalgo); laura.ripoll@ua.es (L. Ripoll).

† Electronic supplementary information (ESI) available: Additional experimental results.

1. Introduction

One of the main challenges of nowadays chemical analysis is to design new analytical devices and procedures able to act as early warning analytical systems, with the aim to provide, in-situ and in real-time, chemical information useful for hazard identification and forecasting for a very broad list of issues of environmental and socioeconomics concern (*e.g.,* pollution threat warning to air or water quality, industrial processes monitoring, food safety surveillance, etc.). To achieve these ambitious objectives, analytical systems should be portable, automatic and able to provide fast analytical information with the required quality for the specific use (fitness for purpose). As a consequence, the trend of today's analytical chemistry is shifting toward the replacement of sophisticated, expensive and bulky laboratory instruments by small-size and fully automated instrumentation useful for field operation.[1]

Laser-induced breakdown spectroscopy technique (LIBS) has particular characteristics that fulfil many of the requirements for acting as an early warning analytical system. LIBS instrumentation can be of small size and completely automatic, with commercially available equipments in a down-scale format already in the market.[2-4] In addition, LIBS measurements are very fast and can be carried out in atmospheric conditions.[5] These special features, with the added advantage of its ability to analyse many different kind of samples without the need of any sample preparation procedure, has made of LIBS an ideal technique for a great number of applications, most of them concerning the direct and *in-situ* analysis of solid and, in a lesser extension, gaseous samples.[6-9] Conversely, the application of LIBS for direct analysis of liquid samples has been traditionally limited by the low sensitivity of the technique, especially for those analytes with high health and environmental impact (*e.g.,* Cd, Cr, Pb, etc.), which are usually detected at concentration levels as high as mg L^{-1} or hundreds of μg L^{-1}.[10-13]

With the aim to overcome the limitation of LIBS analysis of liquids, different strategies involving the use of sample preparation procedures have been investigated by many authors. Among them, it can be cited the absorption or drying of the sample on a solid matrix,[14-18] the application of solid phase extraction (SPE) procedures,[19,20] or the use of modern microextraction procedures in both Liquid-Liquid

Microextraction (LLME)[21-24] and Solid Phase Microextraction (SPME)[25,26] modalities, among others. In general, the use of these sample preparation procedures prior LIBS detection leads to a substantial improvement in the analytical performance of the method, by decreasing the limits of detection at the low μg L^{-1} level. In contrast, since most of the developed sample preparation strategies are not automatic, and/or are difficult to combine with LIBS detection in an automatic way, the implementation of these procedures for real time and *in-situ* applications is hardly feasible. In order to overcome this limitation, a new sample preparation procedure based on the use of electrospray deposition (ESD) is, for the first time, evaluated in this work.

ESD is a relatively mature technique that is becoming more and more popular for the preparation of a great diversity of thin films for many different applications. In ESD, a liquid is forced to flow through a capillary. An electric field is applied between the capillary tip and a grounded substrate. The electrical shear stress elongates the liquid meniscus formed at the outlet of the capillary into a cone and/or a jet, which next deforms and disrupts into fine and highly charged droplets. The repulsive electrostatic interaction forces disperse the droplets homogeneously in the space between the capillary and the substrate, forming a spray which is attracted to the earthed and, if necessary, heated substrate. In this way, the solvent is evaporated near the surface of the heated substrate and the solute in the droplets is deposited as particles onto the surface.[27-31]

ESD is a simple and cheap technique, which permits flexibility to control the film's thickness, the film's uniformity and the amount of substance to be deposited by adjusting different experimental parameters,[27,32] therefore allowing the generation of highly homogeneous and thin films. Moreover, the small size of the generated charged droplets, which are self-dispersed by electrostatic forces, and the fast solvent evaporation, prevent the earlier aggregation of the materials on the substrate, and overcomes the problematic of the inhomogeneous lateral distribution of the solid deposits (*i.e.,* coffee ring effect) usually observed when larger droplets are dried on solids substrates by using the traditional methodology of liquid-to-solid conversion.[22,33] Additionally, electrospray deposition can be easily automated, and the functionality of small-scale ESD devices has been also demonstrated.[34]

Based on the above mentioned considerations, the aim of this work was to evaluate the analytical capabilities of the combination of ESD with LIBS detection for

trace elemental analysis of aqueous samples. To this end, liquid samples were first converted into solids films in an ESD system, and the films were subsequently analysed by LIBS. Three different calibration methodologies were tested for the quantitative analysis of the solid residues by LIBS: (i) external calibration, (ii) conventional standard addition calibration and (iii) on-line standard addition calibration. In all cases, analytical figures of merit of the ESD-LIBS procedure were estimated. A real sample of tap water was used for trueness evaluation by spiking-recovery assays. Results obtained with the proposed ESD-LIBS procedure by using the different calibration methodologies tested were compared and discussed.

2. Experimental

2.1. Instrumentation

2.1.1. LIBS experimental setup

LIBS analysis was performed with the typical LIBS experimental setup shown in Fig. S1†. A Nd:YAG laser (Handy-YAG, model HYL 101, Q-switched, Quanta System S.P.A., Varese, Italy) emitting at its fundamental wavelength (*i.e.,* 1064 nm) with energy 180 mJ per pulse, pulse width of 6 ns FWHM and maximum laser frequency of 10 Hz was used. The laser beam was focused onto the sample by a 60 mm focal length plano-convex lens. The laser spot size on the sample surface, situated at a distance of 60 mm from the focusing lens, was estimated to be ~170 μm diameter, leading to a laser irradiance of ~1.3×10^{11} Wcm^{-2}. Plasma emission was collected at 60° with respect to the laser beam axis by a five-furcated optical fibre (5 × 400 μm fibre optic cable, FC5-UV400-2, Avantes, Eerbeek, The Netherlands), and was sent to the entrance slit of a five-channel spectrometer (AvaSpec-2048-SPU, Avantes, Eerbeek, the Netherlands). LIBS measurements were externally controlled by manually triggering the laser firing (*i.e.,* external triggers to laser flashlamp and Q-switch) with two pulse generators (Digital delay/pulse generator, model DG 535, Stanford Research Systems, Inc., Sunnyvale, USA; and 1 MHz–50 MHz pulse/function generator, model 8116A, Hewlett Packard/Agilent Technologies, Santa Clara, USA). Synchronization of laser firing and data acquisition was performed with the same two-pulse generators system and with the aid of the spectrometer software (AvaSoft©, v 8.5.0.0, Avantes, Eerbeek, The Netherlands). All LIBS spectra were

View Article Online
DOI: 10.1039/C9JA00145J

collected 1.3 μs after the plasma generation, with 1 ms acquisition time. LIBS spectra were processed using a homemade routine running in the Matlab software (Matlab®, v R2009a, The Mathworks, Inc. Natick, USA). The emission lines evaluated were Ni I (352.45 nm), Cd II (214.44 nm) Cr I (359.35 nm) and Zn II (202.55 nm). These lines were selected attending to two different criteria: (i) relative intensity of the emission lines and (ii) spectral interferences (i.e., the selected emission line for a given element was the most intense line among those presenting the minimum spectral interferences with emission lines from the material used as substrate for ESD generation of the solid films).

2.1.2. Electrospray deposition (ESD) system

The ESD system is schematically presented in Fig. 1. The liquid sample was delivered via a syringe pump (model 55-2222, Southnatick Mass 01760, Harvard Apparatus, USA) to a 200 μm inner diameter stainless steel blunt needle. Tygon tubing (Tygon®, R3607 ∅ 0.13 mm, Wertheim, Germany) was used to connect the inlet of the needle to a 100 μL syringe (model 1710RN, Hamilton, Reno, USA) inserted in the syringe pump. The stainless steel needle was connected to a high-voltage unit (Brandenburg LTD, model 2707 Alpha Series II, London, UK) which can generate a DC voltage up to 15 kV. A grounded aluminium plate was placed below the needle and both, the needle and the aluminium plate, were mounted on precision linear translation stages. A manual linear translation stage (Micro-controle/Newport, Evry, France) was used to vertically move the needle in order to precisely adjust the separation distance between the needle tip and the aluminium plate (or deposition substrate) surface (*i.e.,* h distance). The aluminium plate was mounted on an assembly of two linear translation stages for motion in the x-y plane. Motion in the y-axis was performed by a manual linear stage (Orion Corporation, Stamford, USA.), while the x-axis motion was achieved by a programmable, computer-controlled, linear stage (model MFACC linear stage connected to a model CONEX-CC controller, Newport, Irvine, USA). The aluminium plate was heated and temperature-controlled by a heating system consisting of four cartridge heaters and a temperature sensor, all of them embedded in the aluminium block, and a temperature controller (EW4820, Eliwell Controls s.r.l., Belluno, Italy). A flat solid substrate (*i.e.,* an aluminium foil or a glass slide, depending on the experiment) was placed on the grounded aluminium

plate to receive the sprayed sample. The aluminium substrates were standard household aluminium foils, while the glass substrates were 76 x 26 x 1.1 mm microscope slides (Linea LAB S.L., Badalona, Spain). During the spraying process, the electrospray plume was illuminated with the expanded beam of a He-Ne laser (He-Ne Laser, model 30-1, Spindler and Hoyer, Göttingen, Germany) coupled to a 30x beam expander (Newport, Irvine, USA), and the shape and stability of the plume was controlled by visual inspection of the scattered light.

The above described ESD experimental setup was substantially identical for the three calibration methodologies tested in this work (*i.e.,* external calibration, conventional standard addition calibration and on-line standard addition calibration), with the only exception of a different liquid feeding configuration for the on-line standard addition calibration modality. As observed in the upper left inset of Fig. 1, two 50 µL syringes (model 1705RN, Hamilton, Reno, USA) were used in this case, in order to produce the on-line mixing of the sample with the different calibration standards (see Section 3.5 below). The solutions in the syringes were mixed in a Y-shaped connector, and pumped to the stainless steel needle through Tygon tubing.

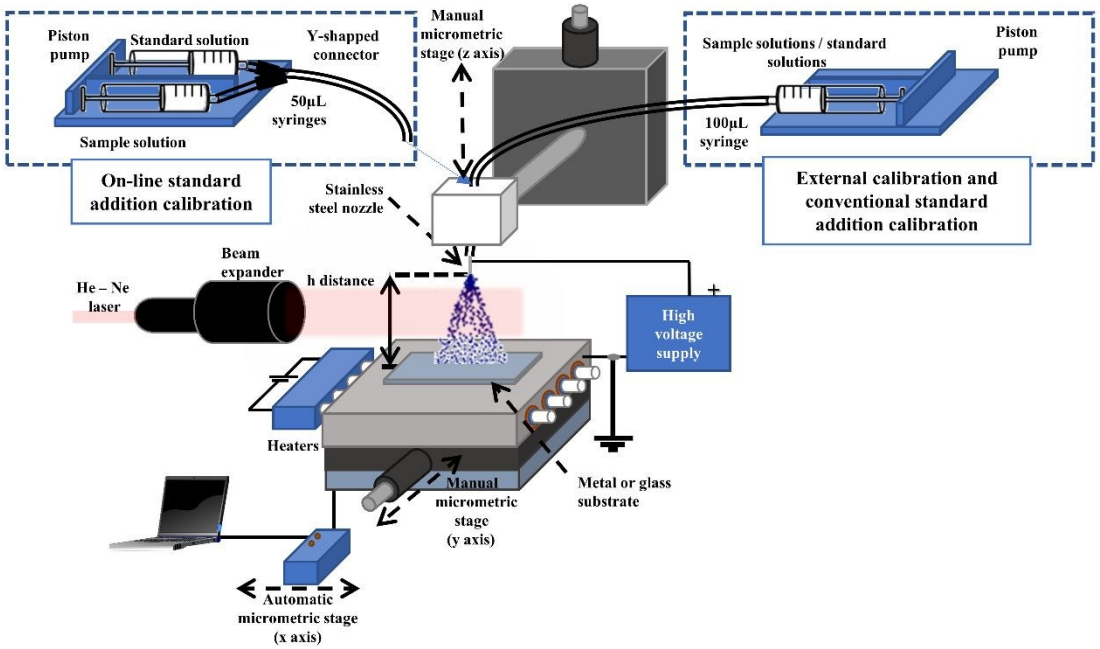

Figure 1: Scheme of the electrospray deposition (ESD) system experimental setup.

2.2. Reagents and solutions

View Article Online
DOI: 10.1039/C9JA00145J

Multi-element aqueous standard solutions at different concentrations were prepared by diluting commercially available mono-element stock solutions of Cd, Cr, Zn and Ni (1000 mg L^{-1} High-Purity Mono-element Standard Solutions, High-Purity Standards, Inc., Charleston, USA) in distilled deionized water (DDW, 18.3 MΩ cm^{-1}). A real sample of tap water, collected from the drinking water supply system of San Vicente del Raspeig in Alicante (Spain), was used for trueness evaluation by spike-recovery experiments. To this end, the sample was previously fortified with the target analytes at a concentration level which depended on the calibration methodology evaluated (*i.e.,* 0.5 mg kg^{-1} for external calibration and conventional standard addition calibration, and 0.4 mg kg^{-1} for on-line standard addition calibration).

2.3. Experimental procedure

The general experimental procedure consisted of two steps: a first one for liquid sample preparation and a second one for LIBS analysis. In the preparation step, the liquid samples were converted into solid films with the use of the ESD system previously described (Section 2.1.2). To this end, after selecting the most appropriate working conditions in the ESD system (Section 3.1 below), 42 µL of solution was electrosprayed onto a solid substrate (*i.e.,* aluminum foil or glass slide, depending on the experiment) at a flowrate of about 6 µL min^{-1}. During the spraying process, the grounded aluminum plate of the ESD system was heated at 180ºC, and it was in continuous movement along the x-axis with the aid of the computer-controlled linear stage, which was programmed to perform forward and reverse cycles of 10 mm travel distance at 2.1 mm s^{-1} translation speed. In these conditions, solid films of approximately 10 mm^2 area were deposited on the substrates, which were subsequently analyzed by LIBS.

Unless otherwise stated, LIBS analysis of the solid residues was carried out by integrating a total of 45 laser shots on the film surface, which were distributed in three different areas (*i.e.,* 15 shots at the center line of the film and 15 shots at each of the edges), as shown in Fig. 2. In these conditions, shot-to-shot variations in emission lines intensities were found to be usually in the range 15-25% RSD. In all cases, the LIBS results presented in this work correspond to the mean integrated intensity of the selected emission lines.

In order to assess the quantitative capability of the proposed ESD-LIBS

methodology, three different calibration approaches were studied: (i) external calibration (Section 3.3), (ii) conventional standard addition calibration (Section 3.4) and (iii) on-line standard addition calibration (Section 3.5). Unless otherwise stated, the presented results are all the mean of three independent replicate measurements.

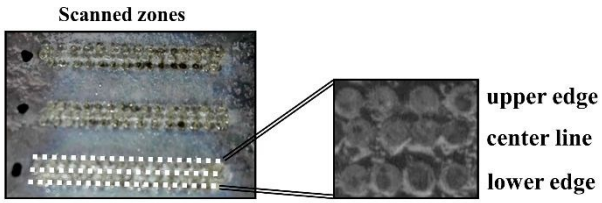

Figure 2: Distribution of laser shots on the surface of solid films obtained by ESD of a model aqueous solution containing 1.0 mg kg^{-1} of the target analytes.

3. Results and discussion

3.1. Selection of the ESD working conditions

In order to select the most appropriate experimental conditions in the ESD system for generation of stable sprays and production of uniform solid films, preliminary deposition studies were performed with the use of a model aqueous solution containing 1 mg kg^{-1} of the different target analytes. In these studies, aluminum foils were used as deposition substrates. The distance between the stainless steel capillary tip and the aluminum substrate (*i.e.,* h distance) was fixed at 7 mm, and the speed and travel distance of the computer-controlled linear stage were kept at 2.1 mm s^{-1} and 10 mm, respectively. Different liquid flowrates (*i.e.,* 4, 6 and 8 µL min^{-1}) and aluminum plate temperatures (*i.e.,* 150, 160, 170 and 180ºC) were evaluated in order to select those conditions maximizing the homogeneity of the generated residues. For each liquid flowrate tested, the applied voltage was adjusted to yield a stable Taylor cone (*i.e.,* electrospray in the cone-jet mode[27-29,31]). After spraying approximately 40 µL of the solution on the aluminum substrate, the generated films were analyzed by visual inspection.

Among the several sample flowrates and aluminum plate temperatures evaluated, the quality of the obtained residues was found to be better when the sample was delivered at 6 µL min^{-1} and the aluminum plate was heated at 180ºC. A

sample flowrate of 4 μL min^{-1} led to difficulties in obtaining a stable cone-jet regime. On the other hand, by increasing the flow rate at 8 μL min^{-1}, inefficient drying of the spray striking the aluminum foil was observed even at the maximum evaluated temperature, leading to inhomogeneous solid residues. When the sample was delivered at 6 μL min^{-1} flowrate, the quality of the films was observed to improve when increasing the aluminum plate temperature from 150ºC to 180ºC. At 150ºC, the liquid solvent was observed to accumulate on the aluminum substrate, ultimately creating a succession of evaporation-driven coffee ring deposits, as can be seen from Fig. 3a. Complete evaporation of the spray on the aluminum substrate was only observed then the aluminum plate temperature was set at 180ºC, leading to more uniform solid films (Fig. 3b).

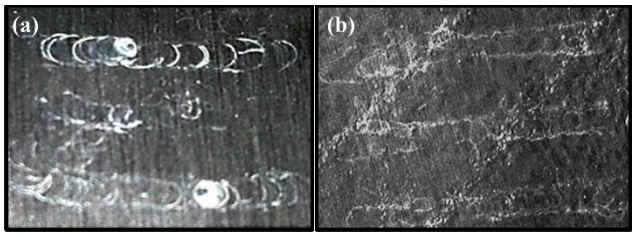

Figure 3: Solid films obtained by spraying a 1.0 mg kg^{-1} model aqueous solution at 6 μL min^{-1} flowrate on aluminum foils heated at (a) 150ºC and (b) 180ºC.

At a liquid flowrate of 6 μL min^{-1} and an h distance of 7 mm, the applied voltage needed to obtain a stable Taylor cone was 5 kV. This cone-jet regime was observed to remain unaffected when the ESD system was tested with several solutions having decreasing analyte concentration (*i.e.,* from 1 mg kg^{-1} to 0.1 mg kg^{-1}). In all cases, the generated residues were nearly identical, as observed from Fig. 4. Thus, the abovementioned ESD working conditions were considered adequate for subsequent experiments.

View Article Online
DOI: 10.1039/C9JA00145J

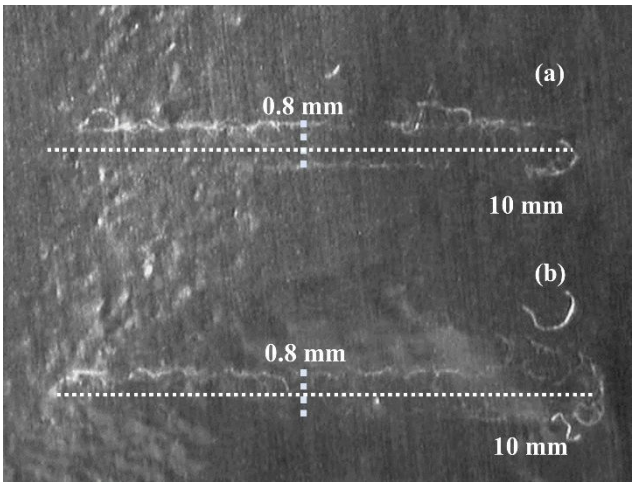

Figure 4: Solid films generated by ESD from model aqueous solutions containing (a) 0.1 mg kg^{-1} of analytes and (b) 1.0 mg kg^{-1} of analytes. ESD conditions: 7 mm h distance, 5 kV applied voltage, 2.1 mm s^{-1} traslational stage speed, 10 mm traslational stage travel distance, 6 µL min^{-1} liquid flowrate, 180ºC aluminum temperature, 7 min deposition time (*i.e.*, 42 µL deposited liquid volume).

3.2. LIBS analysis of the films

After the selection of the ESD experimental conditions, a preliminary test was also performed in order to evaluate the number of in-depth laser shots needed to completely ablate the solid films for LIBS measurements. To this end, a depth-profiling analysis was carried out in a solid residue generated from a model aqueous solution containing 1 mg kg^{-1} of the different target analytes. The solid film was ablated in 30 different positions, with 6 successive laser shots per position. In this depth profiling analysis, aluminum emission lines from the substrate were observed to appear from the first laser shot, and their intensity was observed to remain constant in successive shots, as show in Fig. S2†. Emission intensity from analyte lines, however, were observed to decrease. Fig. 5 shows the decrease in emission intensity obtained for Ni, but similar behavior was observed for the rest of the tested analytes. The data points in the graphic are the mean integrated intensity of Ni I (352.45 nm) emission line over the 30 LIBS measurements performed at each in-depth laser pulse. As observed, the Ni emission signal was drastically reduced after the first laser shot. This fact, and the presence of Al lines from the substrate in the LIBS spectra, led to the conclusion that a practically complete ablation of the film was produced with the first

laser shot. Therefore, only single laser shots at different positions on the surface of the solid residues were performed in all subsequent LIBS measurements.

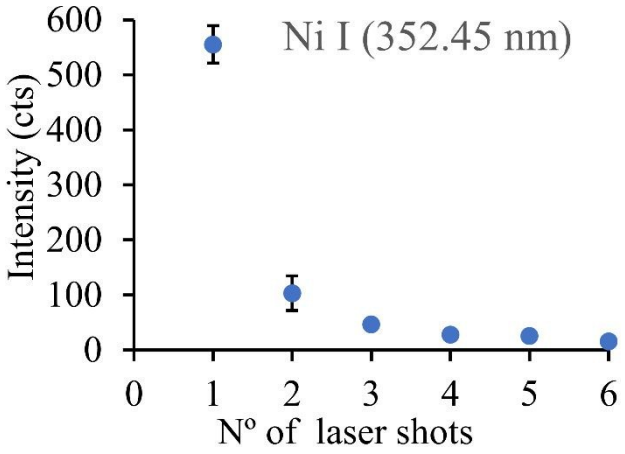

Figure 5: Ni I (352.45 nm) emission line intensity variation in a depth profiling analysis of a solid film obtained by ESD (1.0 mg kg^{-1} model aqueous solution). Results correspond to the mean of 30 LIBS measurements performed at each in-depth laser pulse.

3.3. Evaluation of the ESD-LIBS methodology with the use of the external calibration procedure

The proposed ESD-LIBS methodology was first evaluated with the use of the external calibration approach. To this end, calibration plots were obtained from triplicate analysis of six standard solutions having analyte concentrations ranging from 0.1 to 1 mg kg^{-1}. The solutions were firstly converted into solid in the ESD system, and the resulting solid films were analyzed by LIBS. Different analytical figures of merit were evaluated in order to assess the analytical capability of the procedure.

Results obtained with the use of this calibration methodology are summarized in Table 1. Here, sensitivity was evaluated from the slope of the calibration plots, which are shown in Fig. S3†. LOD and LOQ were calculated following the 3σ and 10σ IUPAC recommendation, respectively, with σ the standard deviation of nine replicate analysis of the less concentrated standard (*i.e.,* 0.1 mg kg^{-1}). Method trueness was evaluated from spike-recovery experiments performed on a real sample of tap water

View Article Online
DOI: 10.1039/C9JA00145J

collected from the municipal water system of the area of San Vicente del Raspeig in Alicante (Spain). As can be observed from Table 1, the obtained LODs and LOQs were at the μg kg^{-1} level for all the tested elements. LODs ranged from 17 μg kg^{-1} for Ni to 57 μg kg^{-1} for Cr, whereas LOQs ranged from 57 μg kg^{-1} to 190 μg kg^{-1} for the same two elements. Linearity was in the range 0.9781 – 0.9977 R^2 for the concentration interval evaluated, and signal repeatability, estimated from the triplicate analysis of the different calibration standards, ranged from about 1% to about 37% RSD (see Fig. S3†). As observed from this figure, signal repeatability was analyte-dependent, with the worst values obtained for Cd and Ni (about 16% and 11% mean RSD, respectively) and the best ones for Zn and Cr (about 9% and 4% mean RSD, respectively).

For method trueness evaluation, the tap water was firstly analysed by ICP-OES in order to estimate the concentration level of the target analytes in the sample. As observed from Table 2, zinc was the only target element detected in tap water by ICP-OES. The concentration level of the other elements was found to be below the limit of detection of the ICP-OES method. In all cases, the concentration level of analytes in the tap water was below the LOD of the proposed ESD-LIBS methodology. After this preliminary study, trueness was evaluated by spiking the sample with 0.5 mg kg^{-1} of the different analytes. Then, un-spiked and spiked samples were analysed in triplicate in order to estimate the recovery for the different metals. As observed from Table 1, unsatisfactory recoveries were obtained for most of the target elements, in especial for Cd, for which the recovery value was as low as 18%. These disappointing results could be attributed to matrix effects arising from morphological differences between the films obtained from the ESD procedure of standard solutions and real samples, with the latter being characterized by a high content of total dissolved solids, as observed from the concentration of major cations in the tap water shown in Table 2. On the one hand, as can be appreciated from the upper right inset in Fig. S4†, the area of the solid residue obtained from ESD of a 0.5 mg kg^{-1} fortified tap water was found to be approximately twice the one obtained from a deionized water standards with the same concentration of analytes (*i.e.*, ~15 mm^2 *vs* ~8 mm^2). This fact probably led to a higher dispersion of the analytes over the surface of the aluminium foil used as substrate and, therefore, to a lower feeding of analytes into the plasma per single laser shot during LIBS analysis. On the other hand, this change in the residues morphology probably led to changes in the ablation mechanism and/or to variations in the

View Article Online
DOI: 10.1039/C9JA00145J

physical parameters of the generated plasmas, as a consequence of a different laser-aluminium substrate interaction. As previously introduced by Aguirre *et al.*,[33] when LIBS experiments are performed on top of a metallic surface, this metallic substrate can contribute to improve the energetic conditions of the generated plasmas, inducing hot and dense plasmas which engulf the rest of the ablated material leading to LIBS signal enhancements (Surface-enhanced LIBS, SENLIBS). Therefore, it can be argued that the lesser the interaction between the laser and the metallic substrate, the lower the surface-enhanced effect. This fact can be appreciated from Fig. S4†, in which the LIBS spectra of a blank aluminium foil, a standard solution residue on the aluminium foil and a tap water residue on the aluminium foil are compared. As observed, the emission intensity of those lines arising from the laser ablation of the aluminium foil (*e.g.*, Al or Fe emission lines) was slightly reduced in the analysis of the standard solution residue, but it was strongly suppressed in the analysis of the tap water residue, indicating a reduction in the ablated aluminium and/or in the energetic conditions of the plasma. Moreover, it can be observed that the intensity of analyte ionic emission lines decreased in the water residue compared to the standard solution, whereas that of atomic emission lines remained practically unaffected or even increased slightly, therefore suggesting a change in the physical parameters of the generated plasmas (see for instance the behaviour of Cr I (359.35 nm) and Cr II (283.56 nm) emission lines).

3.4. Evaluation of the ESD-LIBS methodology with the use of conventional standard addition calibration procedure

Standard addition calibration was tested as an alternative to overcome the matrix effect observed with the external calibration methodology. In these experiments, the same tap water sample fortified with 0.5 mg kg^{-1} of the different analytes was analysed with the standard addition approach. To this end, five even aliquots of 9 g of the fortified sample were spiked with increasing amounts of a 10 mg kg^{-1} multi-element aqueous standard solution, and were rinsed to a final weight of 10 g with deionized water in order to obtain added standard concentrations ranging from 0 to 0.5 mg kg^{-1}. By using the same experimental conditions as in external calibration for both sample preparation and LIBS analysis (see sections 3.1 to 3.3 above), three independent replicate analysis of each solution were carried out in order to obtain

the calibration plots.

Calibration graphs were found to be linear up to 0.3 mg kg^{-1} standard concentration, with R^2 values ranging from 0.9814 to 0.9993 as observed from Fig. S5†. A further increase in the standard concentration led to a decrease in the obtained LIBS signal, probably caused by the occurrence of a morphology variation in the generated ESD film. Fig. 6 shows the ESD films generated from solutions containing 0, 0.3 and 0.5 mg kg^{-1} added standard concentration, along with the entire calibration plot for Zn. As observed, ESD films showing similar morphology were obtained for standard concentrations ranging from 0 to 0.3 mg kg^{-1}, leading to linear response of LIBS signal *vs* analyte concentration. However, when increasing the concentration of the standard to 0.5 mg kg^{-1}, a substantial change in the morphology of the ESD film was appreciated, with the obtained solid residue being characterized by an accumulation of solute along the perimeter of the sprayed area and a practically solute-free central part. This change in the film morphology can be linked to a decrease in the obtained ZnII (202.55 nm) emission line intensity, as observed from the calibration plot in the figure. Similar trend was observed for the rest of the target elements. Thus, the 0.5 mg kg^{-1} concentration standard was finally eliminated from the calibration plots.

Analytical figures of merit evaluated with the use of the conventional standard addition calibration approach are shown in Table 3. Regarding signal repeatability, no substantial differences were observed when compared to the previously studied calibration methodology, with RSD values ranging from 3% to 21% (Fig. S5†). In this case, however, the worst overall RSD values were obtained for Zn and Cd, with 11% mean RSD, and the best one was obtained for Ni (6% mean RSD).

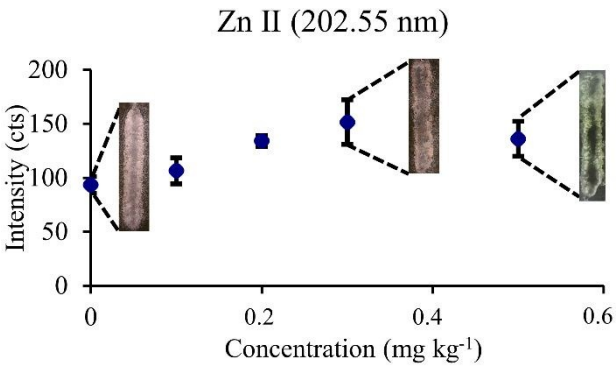

Figure 6: Calibration graph for Zn II (202.55 nm) emission line from 0 to 0.5 mg kg^{-1} added standard concentration,

View Article Online
DOI: 10.1039/C9JA00145J

including photographs of the ESD films obtained for the 0, 0.3 and 0.5 mg kg^{-1} concentration standards.

As predictable from the recovery results obtained with external calibration methodology, sensitivity values were observed to decrease when standard addition calibration was applied. Compared with external calibration (see Table 1 for comparison), sensitivity reduction was specially marked for Cd (*i.e.,* from 517 cts kg mg^{-1} in external calibration to 64 cts kg mg^{-1} in standard addition), and also significant for Zn (*i.e.,* from 630 to 202 cts kg mg^{-1}). On the other hand, only a slight decrease in sensitivity was observed for Cr and Ni.

Despite the reduction in the ESD-LIBS sensitivity for some of the target elements, the overall method trueness was observed to considerably improve with the application of conventional standard addition calibration, as can be seen from the recovery results shown in Table 3. In particular, a substantial improvement was obtained for Cd and Zn, for which recoveries increased from 18% to 110% and from 76% to 100%, respectively, when comparing with external calibration.

3.5. Evaluation of the ESD-LIBS methodology with the use of on-line standard addition calibration procedure

As demonstrated in the previous section, standard addition calibration can offer a valuable alternative for compensation for matrix effects in ESD-LIBS methodology. However, as already well known, conventional standard addition is a slow and tedious procedure, which requires a great many solutions to be prepared and, therefore, could be hardly implemented in automatic measurement systems. In order to overcome these limitations, an alternative on-line standard addition calibration approach was evaluated.

In the on-line calibration method, the overall experimental procedure was similar to that of the previously evaluated methodologies, with only two main differences regarding: (i) the electrospray deposition system setup and (ii) the solid substrate used in the electrospray process.

As already pointed out in the experimental section (Section 2.1.2 above), the liquid feeding configuration of the electrospray system for this calibration methodology consisted in the operation of the piston pump with two 50 μL syringes

(*i.e.,* two liquid inlet channels). In order to perform on-line standard addition calibration, one of the syringes was used to continuously introduce the sample, while the other one was used to sequentially supply calibration standards. After its mixing in a Y-shaped connector, the resulting solution was electrosprayed on a hot substrate to generate the solid film, as in the previous calibration experiments.

In order to assess the precise proportion between sample and standards in the resulting mixtures, a previous calibration procedure of the liquid feeding system was carried out. To this end, the setting of the piston pump was adjusted to deliver a total flowrate after mixing of 6 μL min^{-1}. Then, one of the syringes (namely standard syringe) was filled with a solution containing 2 mg kg^{-1} of all the target analytes plus gallium, while the other one (sample syringe) was filled with a solution containing exclusively 2 mg kg^{-1} of yttrium. Both solutions were mixed in the electrospray system without the application of electric potential, and the resulting mixture was collected at the exit of the stainless steel capillary tip. The experiment was run in triplicate and, finally, originals and mixed solutions were analyzed by ICP-OES. As shown in Fig. S6†, the concentration of all elements in both original solutions was reduced by approximately a half in the mixture, indicating a nearly equal distribution of the total liquid flow between sample and standard channels. From these experiments, a dilution factor of 2.06±0.05 and 1.90±0.12 for sample and standards, respectively, was calculated for the diluted mixture.

For electrospray deposition of the mixed solutions, the aluminum foils used as substrate in the previous calibration experiments were replaced by microscope glass slides, in an attempt to minimize the observed spectral interferences arising from the low purity of the aluminum foils. As can be seen from the LIBS spectra in Fig. S7†, the use of aluminum substrate in LIBS analysis resulted in a more complex and congested spectrum compared to glass, in particular in the spectral regions of the selected Ni and Cr emission lines. In addition, glass slides can be also considered inexpensive and readily available materials, which can be even easier to handle than aluminum foils. As in the previous calibration experiments, 42 μL of solutions were electrosprayed on the glass substrates at a liquid flowrate of 6 μL min^{-1} during a deposition time of 7 min. The settings for the computer-controlled linear stage and the substrate temperature were preserved as in previous measurements, but a different h distance of 13 mm and an applied voltage of 6 kV were needed in order to obtain the cone-jet

View Article Online
DOI: 10.1039/C9JA00145J

regime when using this substrate for ESD.

The on-line standard addition calibration method was tested with the same real sample of tap water used in the preceding studies. Depending on the aim of the experiment (*i.e.,* LOD or trueness evaluation), the sample was previously fortified with 0.1 mg kg^{-1} or with 0.4 mg kg^{-1} of the different analytes. For the acquisition of the standard addition calibration plots, the fortified sample was mixed with four calibration standards having analyte concentrations ranging from 0 to 0.6 mg kg^{-1} (*i.e.,* from 0 to about 0.3 mg kg^{-1} after mixing with the sample in the ESD system), and three replicate measurements were performed. As in the previously evaluated conventional standard addition calibration, a further increase in the calibration standard concentration led to no lineal response in the obtained LIBS emission signal and the resulting calibration graph.

Table 4 summarizes the results obtained with the on-line standard addition calibration method. For LOD and LOQ evaluation, the tap water sample was previously fortified with 0.1 mg kg^{-1} of the different analytes (*i.e.*, approximately 0.05 mg kg^{-1} after mixing with the standards in the ESD system). Five independent calibration plots were obtained, and LOD and LOQ were calculated following the 3σ and 10σ IUPAC criteria. As observed, the results were similar to those obtained with the external calibration methodology (Table 1), with the only difference of a slight decrease in the LODs and LOQs obtained for Cr and Ni.

Trueness was evaluated from the analysis of the tap water sample spiked with 0.4 mg kg^{-1} of analytes (*i.e.*, approximately 0.2 mg kg^{-1} after mixing with the standards in the ESD system). As shown in Fig. S8†, a linear behavior was observed in the added standard concentration interval from 0 to 0.3 mg kg, with R^2 values ranging from 0.9909 to 0.9969. Signal repeatability was between 3% and 16% RSD. No clear correlation was found between the sensitivity values obtained with the on-line and the conventional standard addition calibration methodologies, as can be seen by comparing the data in Table 4 and Table 3. This could be attributed to a combination of two factors: (i) the different dilution of the tap water sample, which leads to variations in the morphology of the solid residues resulting from the ESD process, as pointed out in sections 3.3 and 3.4 above, and (ii) the different influence of the aluminum and glass substrates on the energetic characteristics of the generated LIBS plasmas. In an overall, as observed from Tables 3 and 4, sensitivity increased with the

use of the on-line standard addition calibration only for ionic lines, and decreased or remained practically unaffected for atomic lines. In any case, as observed from Table 4, good recoveries were obtained with the on-line standard addition calibration procedure, with the obtained recovery values ranging between 90% and 105%.

Table 5 compares the results, in terms of LOD, obtained by ESD-LIBS and the on-line standard addition calibration approach with those reported in literature by using similar sample preparation procedures (*i.e.,* sample preparation strategies based on the drying of the liquid sample on a solid substrate). For a proper comparison, a brief description of the different methods is provided in the table, comprising some details on the sample preparation procedure, LIBS instrumentation and measurement conditions. As observed, the proposed ESD-LIBS procedure provides similar or better LODs for all the target analytes compared to other methods, with exception of those reported for Cr and Ni in the work by Niu *et al.*[36] These lower limits of detection, however, were obtained by drying 5 mL of samples on a polished aluminium substrate. That is, with the use of a sample volume nearly 240-fold higher than the one used in ESD-LIBS with the on-line standard addition modality. In addition to the comparatively improved detection limits obtained in the present work, it should be mentioned here that the ESD-LIBS approach is simple, requires a minimum quantity of sample and allows to perform both the liquid sample deposition and its drying in a single and automated step.

4. Conclusions

The results obtained in this work demonstrate that trace elemental analysis of liquids is possible with the proposed ESD-LIBS procedure, which has revealed its suitability for the detection of several analytes of environmental interest in water samples at the low μg kg^{-1} concentration level. Even if sensitive elemental analysis can be successfully achieved with ESD-LIBS, the proposed method has shown to be affected by strong matrix effects, presumably arising from the ESD sample preparation step, which leads to variations in the solid films morphology obtained from samples and standards that induce to changes in the emission signal obtained in subsequent LIBS measurements. This drawback has been effectively corrected with the application of more adequate calibration procedures, such as the traditional or

View Article Online
DOI: 10.1039/C9JA00145J

the on-line standard addition calibration modalities. Compared to external calibration, on-line standard addition calibration has shown to substantially improve the ESD-LIBS method trueness, while preserving the same detection and quantification capabilities. With the application of the on-line standard addition calibration modality, the obtained LODs and LOQs were below 35 μg kg^{-1} and 115 μg kg^{-1}, respectively, for all the analytes under study. Method trueness, evaluated from the analysis of a real sample of tap water characterized by a high hardness level, resulted in recovery values between 90% and 105%.

When ESD-LIBS is compared to previously reported methods for LIBS analysis of liquids using sample preparation procedures based on similar liquid to solid conversion strategies, the proposed ESD-LIBS method provides improved detection and quantification capabilities and requires very low sample consumption. In addition, this method offers a significant advance towards the development of a simple and automatic analytical system for liquid samples analysis based on LIBS: on the one hand, both the ESD and the LIBS detection procedures are easy to automate separately and, on the other hand, the two independent ESD and LIBS processes could be combined in an automatic way without difficulty. Concretely, the use of the on-line standard addition calibration modality with the ESD-LIBS approach can provide sensitive and accurate results in an easily automatable way.

Despite the potential of the proposed ESD-LIBS approach, more research work is still needed in order to extend the currently narrow linear range of the method without degrading its detection capability. This includes: (i) study of the best substrate material to be used in the ESD system for thin film deposition, (ii) study of the most adequate sample dilution and quantity of deposited sample (*i.e.,* optimization of the obtained thin film thickness), or (iii) application of the μ-LIBS modality to the analysis of the solid residues. These possible ways for improvement are currently under study in our laboratory.

Conflicts of interest

There are no conflicts of interest to declare.

Acknowledgements

View Article Online
DOI: 10.1039/C9JA00145J

L. Ripoll is grateful to the Ministry of Economy and Competitiveness for her PhD fellowship (FPI-MICINN (BES-2012-058759)).

References

1. F. Pena-Pereira, in *Miniaturization in Sample Preparation*, ed. F. Pena-Pereira, De Gruyter Open Ltd, Berlin, 1st edition, 2014, chapter 1, 1-28.
2. *Marwan Technology*, http://www.marwan-technology.com/en/products/analytical-instrumentation/libs/, (accessed March 2019).
3. *TSI Inc.*, http://www.tsi.com/ChemLite-Portable-LIBS-Metal-Analyzer/, (accessed March 2019).
4. *Stellar Net Inc.*, http://www.stellarnet.us/systems/porta-libs-2000-and-plasma-monitor-configurations/, (accessed March 2019).
5. D. A. Cremers and L. J. Radziemski, in *Handbook of Laser Induced Breakdown Spectroscopy*, John Wiley & Sons Ltd, West Sussex, 2nd edition, 2013.
6. A. Cousin, V. Sautter, V. Payré, O. Forni, N. Mangold, O. Gasnault, L. L. Deit, J. Johnson, S. Maurice, M. Salvatore, R. C. Wiens, P. J. Gasda and W. Rapin, *Icarus*, 2017, **288**, 265-283.
7. W. Rapin, B. Chauviré, T. S. J. Gabriel, A. C. McAdam, B. L. Ehlmann, C. Hardgrove, P. Y. Meslin, B. Rondeau, E. Dehouck, H. B. Franz, N. Mangold, S. J. Chipera, R. C. Wiens, J. Frydenvang and S. Schröder *J. Geophys. Res. Planets*, 2018, **123**, 1955–1972.
8. R. Noll, C. Fricke-Begemann, S. Connemann, C. Meinhardt and V. Sturm, *J. Anal. At. Spectrom.*, 2018, **33**, 945–956.
9. Y. Wu, M. Gragston, Z. Zhang, P. S. Hsu, N. Jiang, A. K. Patnaik, S. Roy and J. R. Gord, *Combust. Flame*, 2018, **198**, 120–129.
10. V. Lazic, in *Laser induced breackdown spectroscopy. Springer Series in Optical Sciences 182*, ed. S. Musazzi and U. Perini, Springer-Verlag, Berlin, 1st edition, 2014, chapter 8, 195–225.
11. V. Lazic and S. Jovićević, *Spectrochim. Acta B*, 2014, **101**, 288-311.
12. X. Yu, Y. Li, X. Gu, J. Bao, H. Yang and l. Sun, *Environ. Monit. Assess.*, 2014, **186**, 8969–80.

13. S. L. Zhong, Y. Lu, W. J. Kong, K. Cheng and R. Zheng, *Front. Phys.*, 2016, **11**, 114202.

14. Z. Chen, Y. Godwal, Y. Y. Tsui and R. Fedosejevs, *Appl. Opt.*, 2010, **49**, C87–C94.

15. A. Sarkar, S. K. Aggarwal, K. Sasibhusan and D. Alamelu, *Microchim. Acta*, 2010, **168**, 65–69.

16. Q. Lin, Z. Wei, M. Xu, S. Wang, G. Niu, K. Liu, Y. Duan and J. Yang, *RSC Adv.*, 2014, **4**, 14392–14399.

17. Q. Shi, G. Niu, Q. Lin, X. Wang, J. Wang, F. Bian and Y. Duan, *J. Anal. At. Spectrom.*, 2014, **29**, 2302–2308.

18. N. Aras and Ş Yalçın, *Talanta*, 2016, **149**, 53–61.

19. A. F. M. Y. Haider, M. H. Ullah, Z. H. Khan, F. Kabir and K. M. Abedin, *Opt. Laser Technol.*, 2014, **56**, 299–303.

20. X. Wang, Y. Wei, Q. Lin, J. Zhang and Y. Duan, *Anal. Chem.*, 2015, **87**, 5577–5583.

21. M. Aguirre, E. Selva, M. Hidalgo and A. Canals, *Talanta*, 2015, **131**, 348–353.

22. M. A. Aguirre, H. Nikolova, M. Hidalgo and A. Canals, *Anal. Methods*, 2015, **7**, 877–883.

23. I. Gaubeur, M. Aguirre, N. Kovachev, M. Hidalgo and A. Canals, *Microchem. J.*, 2015, **121**, 219–226.

24. I. Gaubeur, M. A. Aguirre, N. Kovachev, M. Hidalgo and A. Canals, *J. Anal. At. Spectrom.*, 2015, **30**, 2541–2547.

25. X. Wang, L. Shi, Q. Lin, X. Zhu and Y. Duan, *J. Anal. At. Spectrom.*, 2014, **29**, 1098–1104.

26. F. Ruiz, L. Ripoll, M. Hidalgo and A. Canals, *Talanta*, 2019, **191**, 162–170.

27. I. B. Rietveld, K. Kobayashi, H. Yamada and K. Matsushige, *J. Phys. Chem. B*, 2006, **110**, 23351–23364.

28. A. Jaworek, *J. Mater. Sci.*, 2007, **42**, 266–297.

29. A. Jaworek and A. T. Sobczyk, *J. Electrost.*, 2008, **66**, 197–219.

30. Y. Matsushima, Y. Nemoto, T. Yamazaki, K. Maeda and T.Suzuki, *Sens. Actuators, B*, 2003, **96**, 133–138.

31. J. Rosell-Llompart, J. Grifoll and I. G. Loscertales, *J. Aerosol Sci.*, 2018, **125**, 2–31.

32. S. Roncallo, J. D. Painter, S. A. Ritchie, M. A. Cousins, M. V. Finnis and K. D. Rogers, *Thin Solid Films*, 2010, **518**, 4821– 4827.

33. M. A. Aguirre, S. Legnaioli, F. Almodóvar, M. Hidalgo, V. Palleschi and A. Canals, *Spectrochim. Acta B*, 2013, **79-80**, 88-93.

34. J. Ju, Y. Yamagata and T. Higuchi, *Adv. Mater.*, 2009, **21**, 4343–4347.

35. L. Fang, N. Zhao, M. Ma, D. Meng, Y. Jia, X. Huang, W. Liu and J. Liu, *Plasma Sci. Technol.,* 2019, **21**, 034002.

36. S. Niu, L. Zheng, A. Q. Khan, G. Feng and H. Zeng, *Talanta*, 2018, **179**, 312-317.

37. M. Bukhari, M. A. Awan, I. A. Qazi and M. A. Baig, *J. Anal. Methods Chem*., 2012, **2012**, 823016.

38. D. Meng, N. Zhao, Y. Wang, M. Ma, L. Fang, Y. Gu, Y. Jia and J. Liu, *Spectrochim. Acta B*, 2017, **137**, 39-45.

39. C. Chen, G. Niu, Q. Shi, Q. Lin and Y. Duan, *Appl. Opt.*, 2015, **54**, 8318–8325.

View Article Online
DOI: 10.1039/C9JA00145J

Tables

Table 1. Analytical figures of merit obtained with the use of the ESD-LIBS methodology by applying the external calibration approach

Emission Line (nm)	Sensitivity[a] (cts kg mg^{-1})	LOD[b] (µg kg^{-1})	LOQ[b] (µg kg^{-1})	Trueness evaluation in tap water sample (analyte concentration in mg kg^{-1})[c]		
				Added	Found	Recovery (%)
Zn II (202.55 nm)	630 ± 40	30	100	0.49	0.37 ± 0.07	76
Cd II (214.44 nm)	517 ± 12	19	62	0.49	0.09 ± 0.02	18
Cr I (359.35 nm)	990 ± 60	57	190	0.50	0.61 ± 0.06	123
Ni I (352.45 nm)	560 ± 30	17	57	0.51	0.57 ± 0.05	112

[a] Slope on the calibration curve.
[b] Calculated according to the 3σ (LOD) and 10σ (LOQ) criteria, with σ the standard deviation of 9 different replicate measurements of the most diluted standard (0.1 mg kg^{-1}).
[c] Evaluated from three independent replicate measurements of the tap water sample spiked with ~ 0.5 mg kg^{-1} of analytes.

View Article Online
DOI: 10.1039/C9JA00145J

Table 2. Concentration of some mayor and trace cations in the real tap water sample obtained by ICP-OES analysis, along with the ICP-OES experimental measurement conditions

Operational parameters	
RF applied power (kW)	1.2
Outer gas flow rate (L min^{-1})	15
Auxiliar gas flow rate (L min^{-1})	1.5
Nebulizer	OneNeb®
Spray chamber	Cyclonic-type
Nebulizer gas flow rate (L min^{-1})	0.75
Sample uptake rate (mL min^{-1})	1.5
Number of replicates	5
Viewing mode	Axial
Analytical emission lines (nm)	Ca II (422.673) Na I (589.592) Mg II (279.553) Zn II (202.548) Cd II (214.439) Cr I (357.868) Ni I (231.604)
Major Components	
Ca II (422.673) (mg kg^{-1})	135 ± 8
Na I (589.592) (mg kg^{-1})	107 ± 5
Mg II (279.553) (mg kg^{-1})	72 ± 5
Trace Components	
Zn II(202.548) (mg kg^{-1})	0.019 ± 0.002
Cd II (214.439) (mg kg^{-1})	a
Cr I (357.868) (mg kg^{-1})	a
Ni I (231,604) (mg kg^{-1})	a

a Below the LOD of the ICP-OES method.

View Article Online
DOI: 10.1039/C9JA00145J

Table 3. Analytical figures of merit obtained with the use of the ESD-LIBS methodology by applying the conventional standard addition calibration approach

Emission Line (nm)	Sensitivity[a] (cts kg mg^{-1})	Trueness evaluation in tap water sample (analyte concentration in mg kg^{-1})[b]		
		Added	Found	Recovery (%)
Zn II (202.55 nm)	202 ± 19	0.50	0.50 ± 0.06	100
Cd II (214.44 nm)	64 ± 3	0.50	0.55 ± 0.04	110
Cr I (359.35 nm)	850 ± 80	0.51	0.51 ± 0.07	100
Ni I (352.45 nm)	514 ± 10	0.51	0.464 ± 0.012	91

[a] Slope on the calibration curve.
[b] Evaluated from the analysis of three independent replicate measurements of the tap water sample spiked with ~ 0.5 mg kg^{-1} of analytes.

View Article Online
DOI: 10.1039/C9JA00145J

Table 4. Analytical figures of merit obtained with the use of the ESD-LIBS methodology by applying the on-line standard addition calibration approach

Emission Line (nm)	Sensitivity[a] (cts kg mg^{-1})	LOD[b] (µg kg^{-1})	LOQ[b] (µg kg^{-1})	Trueness evaluation in tap water sample (analyte concentration in mg kg^{-1})[c]		
				Added	Found	Recovery (%)
Zn II (202.55 nm)	362 ± 17	31	102	0.41	0.42 ± 0.04	102
Cd II (214.44 nm)	214 ± 8	12	38	0.40	0.41 ± 0.03	103
Cr I (359.35 nm)	360 ± 20	34	112	0.41	0.43 ± 0.04	105
Ni I (352.45 nm)	500 ± 30	9	30	0.39	0.35 ± 0.05	90

[a] Slope on the calibration curve.
[b] Calculated according to the 3σ (LOD) and 10σ (LOQ) criteria, with σ the standard deviation of 5 different replicate measurements of a tap water sample spiked with 0.1 mg kg^{-1} of the different analytes.
[c] Evaluated from three independent replicate measurements of the tap water sample spiked with ~ 0.4 mg kg^{-1} of analytes.

Table 5. Comparison of the limits of detection obtained in the present work with those reported in literature by using a similar sample preparation strategy

Brief description of the method	LODs (μg L^{-1}) / Emission line	Reference
Sample preparation: drying of 16 μL sample on an annular groove performed on hydrophilic graphite flakes. The sample is transferred to the substrate by manual dripping. LIBS equipment: laser Nd:YAG - λ 1064 nm, E 100 mJ, τ 6 ns, f 2 Hz. Detection system - multichannel modular spectrograph with linear CCD arrays. Measurement conditions: mean of 3 replicate measurements. Accumulation of 40 single shots per measurement. External calibration.	Zn (49) / Zn I (213.86 nm) Cd (29) / Cd II (214.44 nm) Cr (87) / Cr I (425.43 nm) Ni (83) / Ni I (341.48nm)	35
Sample preparation: drying of 1 mL (or 5 mL) sample on a polished aluminium target surface. The sample is transferred to the substrate by manual dripping. LIBS equipment: laser Nd:YAG - λ 1064 nm, E 60 mJ, τ 5 ns, f 5 Hz. Detection system - Echelle spectrograph with ICCD detector. Measurement conditions: mean of 7 replicate measurements. Accumulation of 70 single shots per measurement. External calibration.	LODs for (1 mL | 5 mL) sample Zn (NE) Cd (184 | 24.7) / Cd I (508.58 nm) Cr (19 | 3.48) / Cr I (425.43 nm) Ni (22 | 5.38) / Ni I (341.48 nm)	36
Sample preparation: drying of 0.5 μL sample on a 300nm oxide coated silicon wafer substrate (Si + SiO_2). The sample is transferred to the substrate by manual dripping. LIBS equipment: laser Nd:YAG - λ 532 nm, E 200 mJ, τ 10 ns, f manual laser firing. Detection system - Echelle spectrograph with ICCD detector. Measurement conditions: mean of 5 replicate measurements. One single shot per measurement. External calibration.	Zn (NE) Cd (158) / Cd II (226.50 nm) Cr (NE) Ni (NE)	18
Sample preparation: drying of 0.5 mL of sample on absorption papers for Petri. The sample is transferred to the substrate by manual dripping. LIBS equipment: laser Nd:YAG - λ 1064 nm, E 89.5 mJ (Cd) and 146.7 (Cr), τ 10 ns, f 10 Hz. Detection system - multichannel spectrometer with CCD detectors. Measurement conditions: mean of 10 replicate measurements. Accumulation of 20 single shots per measurement. External calibration.	Zn (NE) Cd (46000) / Cd II (226.50 nm) Cr (230000) / Cr I (427.48 nm) Ni (NE)	37
Sample preparation: drying of 100 μL of sample on electrospun ultrafine fibers. The sample is transferred to the substrate by manual dripping. LIBS equipment: laser Nd:YAG - λ 1064 nm, E 40 mJ, τ 6 ns, f 10 Hz. Detection system - Echelle spectrograph with EMCCD detector.	Cr (1800) / Cr I (425.43 nm)	16

Measurement conditions: mean of 10 replicate measurements. Accumulation of 100 single shots per measurement. External calibration.		
Sample preparation: drying of 100 µL of sample on 3D anodic aluminium oxide porous membrane. The sample is transferred to the substrate by manual dripping. LIBS equipment: laser Nd:YAG - λ 1064 nm, E 210 mJ, τ 6 ns, f 10 Hz. Detection setup: Echelle spectrograph with EMCCD detector. Measurement conditions: mean of 10 replicate measurements. Accumulation of 50 single shots per measurement. External calibration.	Cr (110) / Cr I (427.48 nm)	17
Sample preparation: drying of the sample on a groove performed in the middle of a graphite sheet. Volume of sample: NI. The sample is transferred to the substrate by manual dripping. LIBS equipment: laser Nd:YAG - λ 1064 nm, E 100 mJ, τ 5 ns, f NI. Detection system: multichannel modular spectrograph with linear CCD arrays. Measurement conditions: Replicate measurements and number of accumulated laser shots per measurement NI. External calibration.	Zn (180)[a] / emission line NI. Cd (62)[a] / Cd II (214.44 nm) Cr (33)[a] / emission line NI. Ni (44)[a] / Ni I (352.45 nm)	38
Sample preparation: drying of 200 µL of sample on plant fiber spunlaced nonwovens. The sample is transferred to the substrate by manual dripping. LIBS equipment: laser Nd:YAG - λ 1064 nm, E 238 mJ, τ 6 ns, f 2 Hz. Detection system: Echelle spectrograph with EMCCD detector. Measurement conditions: mean of 10 replicate measurements. Accumulation of 100 single shots per measurement. External calibration.	Cr (700) CrI (427.48 nm) Ni (5700) NiI (352.45 nm)	39
Sample preparation: drying of 42 µL of mixture (sample + standards (1:1)) on microscope glass slides. The sample is transferred to the substrate by an automatic electrodeposition system. LIBS equipment: laser Nd:YAG - λ 1064 nm, E 180 mJ, τ 6 ns, f manual firing. Detection system: multichannel modular spectrograph with linear CCD arrays. Measurement conditions: mean of 3 replicate measurements. Accumulation of 45 single shots per measurement. On-line standard addition calibration.	Zn (31)[a] / Zn II (202.55 nm) Cd (12)[a] / Cd II (214.44 nm) Cr (34)[a] / Cr I (359.35 nm) Ni (9)[a] / Ni I (352.45 nm)	This work

λ laser wavelength; E laser energy per pulse; τ laser pulse width; f laser frequency
NI not indicated; NE not evaluated
[a] LOD expressed as µg kg^{-1}